Published in: Angiogenesis (2001), vol. 4, iss. 2, pp. 133-142
Status: Postprint (Author's version)

Improved quantification of angiogenesis in the rat aortic ring assay

Silvia Blacher[1,*], Laetitia Devy[1,*], Mike F. Burbridge[2], Guy Roland[1], Gordon Tucker[2], Agnes Noël[1] & Jean-Michel Foidart[1]
Laboratory of Tumor and Developmental Biology, University of Liège, Tour de Pathologie +3, CHU, Sart-Tilman, Liège, Belgium; Experimental Oncology Division, Institut de Recherches Servier, Suresnes, France

ABSTRACT

In vitro angiogenesis assays are essential for the identification of potential angiogenic agents and screening for pharmacological inhibitors. Among these assays, the rat aortic ring model developed by Nicosia bridges the gap between *in vivo* and *in vitro* models. The quantification of angiogenesis on this system must be applicable to characterise vascular networks of various states of complexity. We present here an improved computer-assisted image analysis which allows: (1) the determination of the aortic ring area and its factor shape; (2) the number of microvessels, the total number of branchings, the maximal microvessel length and the microvessel distribution; (3) the total number of isolated fibroblast-like cells and their distribution. We show that this method is suitable to quantify spontaneous angiogenesis as well as to analyse a complex microvascular network induced by various concentrations of vascular endothelial growth factor (VEGF). In addition, by evaluating a new parameter, the fibroblast-like cell distribution, our results show that: (1) during spontaneous angiogenic response, maximal fibroblast-like cell migration delimits microvascular outgrowth; and (2) the known angiogenic inhibitor Batimastat prevents endothelial cell sprouting without completely blocking fibroblast-like cell migration. Finally, this new method of quantification is of great interest to better understand angiogenesis and to test pro- or anti-angiogenic agents.

Key words*:* angiogenesis, image analysis, protease inhibitors, rat aortic ring model, VEGF

INTRODUCTION

Angiogenesis, the development of new blood vessels, is an essential feature of tissue remodelling and wound healing [1]. In adults, the most important angiogenesis-dependent diseases are associated with the growth of solid tumours, proliferative retinopathies, and rheumatoid arthritis [2, 3]. Consequently, extensive interests are generated in the molecular mechanism elucidation of vessel growth. The angiogenic process is regulated both by positive and negative factors that modulate the migration, proliferation, proteolytic activity and differentiation of endothelial cells. Various *in vivo* and *in vitro* models have been developed in order to test the effect of angiogenic agonists or antagonists, and to investigate the cellular and molecular mechanisms of angiogenesis. *In vivo* assays can be complicated by inflammatory reactions resulting in the release of angiogenic cytokines from inflammatory cells. On the other hand, *in vitro* models, with isolated endothelial cells are useful, but most angiogenic factors stimulate endothelial cell motility and proliferation, without inducing microvascular sprouting, branching and capillary tube formation. These systems represent only a partial reconstruction of the vascular wall and paracrine interactions between endothelial cells and perivascular cells such as pericytes, smooth muscle cells or fibroblasts [4]. The aorta ring assay developed initially by Nicosia and Ottinetti [5] bridges the gap between *in vivo* and *in vitro* models. In this system, rat aortic rings cultured in collagen gel give rise to microvascular networks composed of branching endothelial channels. By using intact vascular expiants, it reproduces more accurately the environment in which angiogenesis takes place than those with isolated endothelial cells. The quantification of angiogenesis on this system implies the determination of the following geometric and morphologic parameters: (1) number and length of branching microvessels; (2) size and form of aortic rings; and (3) number and spatial distribution of fibroblast-like cells.

To our knowledge, quantification on the aortic ring model has been performed according to the three following approaches: (1) manual processing and measurement [5-7]; (2) global characterisation [8, 9]; and (3) automatic binary processing of grey level image and determination of the number and the total area of microvessels at a fixed distance from the aortic ring [10]. Those kinds of quantification suffer from a number of practical

* The first two authors contributed equally to the present work

difficulties. Mainly manual processing is slow, annoying and subjective. By comparison with the first ones, Nissanov et al. [10] approach presents the great advantages of being fully automatic and well adapted to the screening of anti-angiogenic molecules. Nevertheless, as noticed by the authors themselves, the more accurate procedure, i.e., the vessel area determination, cannot allow distinguishing between increased vessel length and increased vessel number.

The aim of the present study is to validate the sensitivity of an improved image-processing algorithm, which allows extracting vessels and fibroblast-like cells during spontaneous or modulated angiogenesis, by the determination of additional relevant parameters.

MATERIALS AND METHODS

Rat aorta ring assay

Angiogenesis was studied by culturing aortic expiants in three-dimensional matrix gels according to the procedure of Nicosia and Ottinetti [5]. Thoracic aortas were removed from 8- to 12-week-old male fisher-344 rats immediately transferred to a culture dish containing cold serum-free minimum essential medium (MEM, Life Technologies Ltd., Paisley, Scotland). The periaortic fibroadipose tissue was carefully removed with fine microdissecting forceps and iridectomy scissors paying special attention not to damage the aortic wall. One millimetre-long aortic rings (approximately 20 per aorta) were sectioned and extensively rinsed in five consecutive washes of MEM medium. Ring-shaped expiants of rat aorta were then embedded in gels of rat tail interstitial collagen (1.5 mg/ml) as previously described by Montesano et al. [11]. The final collagen solution was obtained by mixing 7.5 volumes of collagen (2 mg/ml) (Collagen R, Serva, Heidelberg, Germany) with 1 volume of 10 × MEM, 1.5 volumes of $NaHCO_3$ (15.6 mg/ml) and approximately 0.1 volume NaOH (1 M) to adjust the pH to 7.4. The collagen gel cultures were first prepared in cylindrical agarose wells [5] and kept in triplicates at 37 °C in 100 mm diameter Petri dishes (bacteriological polystyrene, Falcon, Becton Dickinson, Lincoln Park, New Jersey): each dish con-tained 30 ml of MCDB131 medium (Life Technologies Ltd, Paisley, Scotland), supplemented with 25 mM $NaHCO_3$, 1% glutamin, 100 U/ml penicillin and 100 µg/ml streptomycin. The cultures were kept at 37 °C in a humidified environment for 2 weeks and examined every second days by phase contrast micros-copy with an Olympus microscope at the appropriate magnification. Image analysis was performed on a Workstation Sun SPARC30, using the software 'Visilog5.0' from Noesis. Images were digitised in 760 x 540 pixels with 256 grey levels. Grey level image transformation and binary image processing have been carrying out using traditional tools and mathematical morphology [12]. Testing was conducted by using at least triplicate culture per condition.

The identification of endothelial cells was based on their ability to uptake low-density lipoprotein (LDL). Prior to sectioning, and collagen embedding, aortas were incubated for 4 h at 37 °C in a solution of 10 μg/ml acetylated-LDL labelled with the fluorescent probe 1,1'-dioctadecyl-3,3,3',3'-tetramethyl-indocarbocyanine per-chlorate (Dil-Ac-LDL) (Biomedical Technologies Inc., Stoughton, Massachussets) [13]. Cultures were then examined by fluorescent microscopy using rhodamine excitation and emission filters. Aortic ring and microvascular endothelial cells were fluorescent whereas the intensity of fibroblast-like cells (smooth muscle cells and pericytes) was only slightly above background levels.

Preparation and addition of test drugs

In some assays, the aortic outgrowth was evaluated in the presence of vascular endothelial growth factor (VEGF, Sigma) added to the culture medium (5-20 ng/ml) immediately after aortic ring embedding. A broad-spectrum hydroxamic acid based synthetic inhibitor of matrix metalloproteinases (Batimastat) from British Biotech (British Pharmaceuticals, Oxford, United Kingdom) was tested. Batimastat (10^{-9}-10^{-6} M) or DMSO alone as vehicle (0.1%) was added to the culture medium after aortic ring embedding. In order to adjust pH to 7.4, culture medium was equilibrated with bicarbonate.

Statistical analysis

The following statistical parameters have been calculated to describe the distribution of microvessels (N_i) and fibroblast-like cells (N_f) [14]: (1) the mean distribution ($\overline{D}$), and the standard deviation; (2) the mode (d); (3) the skewness (sk), which describes the symmetry of the distribution (sk = 0 for symmetrical distributions, sk < 0 or sk > 0 for asymmetrical distributions with the longer 'tail' of the curve to the left or to the right, respectively); and (4) the kurtosis (k) which describes how flat or peaked the distribution is (k = 0 for a gaussian distribution, k < 0 for a flat distribution and k > 0 for a peaked one). In our study, $\overline{D}$ corresponds to the distance from the

Published in: Angiogenesis (2001), vol. 4, iss. 2, pp. 133-142
Status: Postprint (Author's version)

expiant at which N_i or N_f reach its mean value, *d* corresponds to the distance from the expiant at which most cells migrated, a positive sk value indicates that most cells migrate at distances lower than $\overline{D}$ and *k* indicates the cell dispersion around *d.* The same scale of distance has been used in all the histograms in order to facilitate the comparison between different cases.

Figure 1. *Binary image processing of a typical aortic ring with endothelial cells organised as branching microvessels surrounded by isolated fibroblast-like cells.* Panel a: normalisation of the original grey levels between 0 and 256. Panels b, c, aortic ring extraction: application of a morphologic low-pass filter (panel b) and threshold transformation (panel c). Panels d-h, microvessel and fibroblast-like cells extraction: logical subtraction of images (panel d); threshold transformation into binary image (panel e), hole-fill transformation and border elimination (panel f); filtering and logical subtraction leading to obtain microvessels (panel g) and fibroblast-like cells (panel h) images.

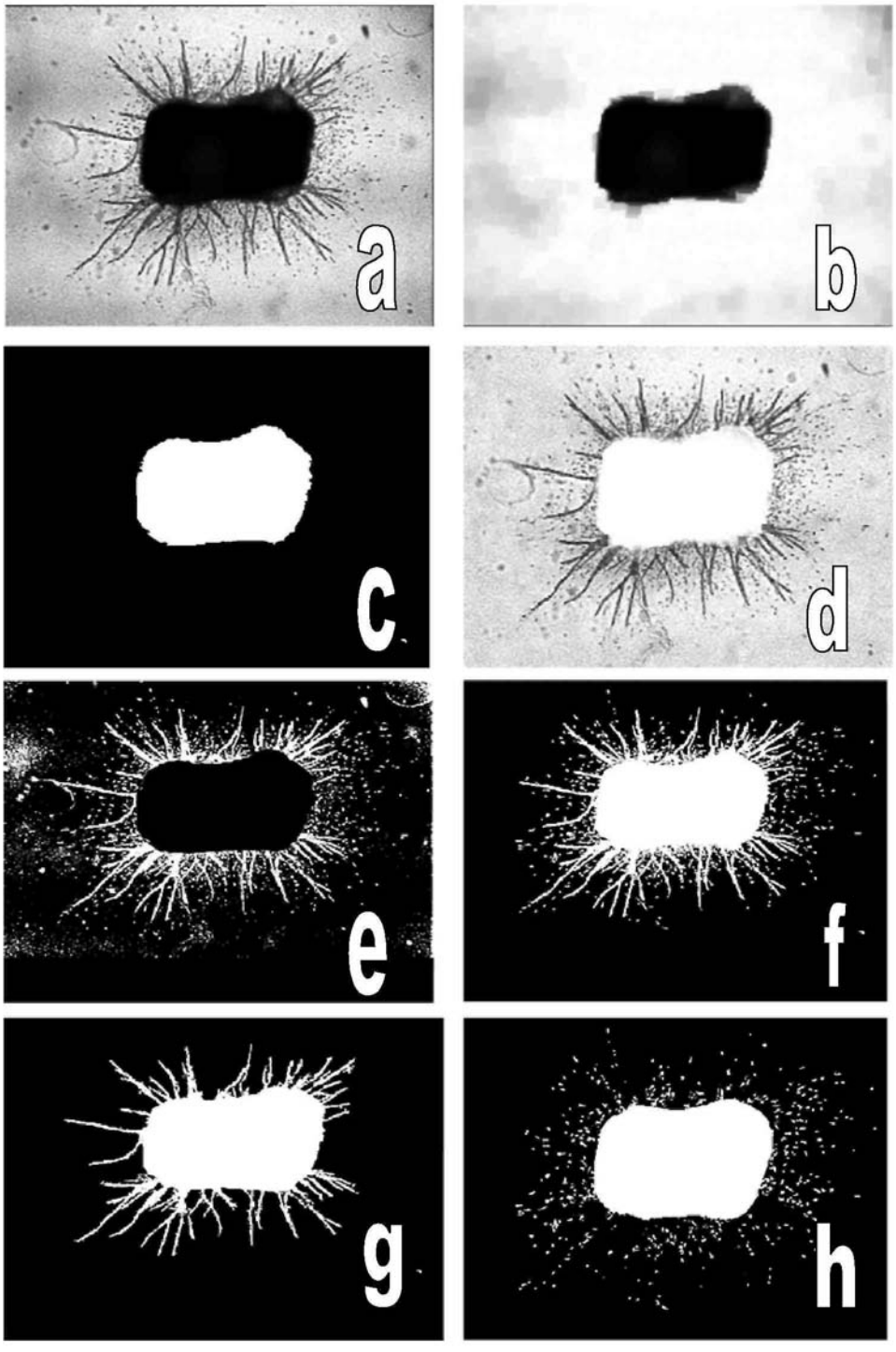

Published in: Angiogenesis (2001), vol. 4, iss. 2, pp. 133-142
Status: Postprint (Author's version)

RESULTS

Image processing

Imaging set-up

Figure la shows a typical image of an aortic ring at day 10 of culture, giving rise to branching microvessels, surrounded by elongated fibroblast-like isolated cells. Ideally, sample preparation, optical microscopy observations and image caption conditions must be carefully established in order to achieve optimum image quality, i.e., and a maximum contrast between the sample and the background. However, experimental conditions prevent, in some cases, to fulfill completely this requirement. For example, if the aortic ring is placed at the border of the support, uneven illumination could generate a dark rim on both sides of the image. Moreover, before binary image measurements, some artefacts (air bubbles, dirt) are usually observed. Under these conditions, the setting of grey level transformations is a necessary step to improve the quality of the image.

Binary image processing

The binary image has been performed by a two step procedure (Figure 1). After normalisation of original grey level images between 0 and 256 (Figure 1a), aortic ring extraction, on one hand, and microvessels and fibroblast-like cells extraction, on the other hand, were achieved. For aortic ring extraction, a morphologic low-pass filter was first applied to smooth the background and to eliminate microvessels and fibroblast-like cells (Figure 1b). Then, a threshold transformation led to a binary image. Finally, opening and border elimination transformations are applied to exclude artefacts (Figure 1c). For microvessels and fibroblast-like cells, a logical subtraction of images was first applied to eliminate the aortic ring (Figure 1d). Then, threshold transformation into binary image (Figure le), hole-fill transformation and border elimination to exclude artefacts were carried out (Figure 1f). Finally, a filtering and a logical subtraction allowed obtaining microvessel (Figure 1g) and fibroblast-like cell (Figure 1h) images. It must be noticed that most of these transformations are parameter dependent. As a rule, if all images were digitised under the same conditions, parameters were fixed once for ever, and images binary processing was then completely automatic. The algorithm used here can be easily implemented on any computer including appropriate image analysis software. The time of processing images and measurements depended on the available computer system.

Measured parameters

After generation of binary image, the following automatic measurements were performed: (1) the aortic ring area defines the area of the projection of the aortic ring into the image (A) and its factor shape (F). A (mm^2) = number of pixels which form the object × a calibration constant square. F = perimeter$^2/4\pi A$, which describes the deviation of an object from a true circle. It gives a minimal value of 1 for a circle and larger values for shapes having a higher ratio of perimeter to area; (2) the quantification of microvessels according to the vascular network complexity, i.e., in all cases, the determination of the microvessel distribution (N_i), and, when applicable, the determination of the number of microvessels (N_v), the total number of branching (N_b), and the maximal microvessel length (L_{max}); (3) the total number of isolated fibroblast-like cells (N_f).

In relation to microvascular network complexity, two situations have been encountered: spontaneous and induced-angiogenesis.

(a) Spontaneous angiogenesis: in this case, each microvessel, with its branching can be clearly identified. The number of microvessels (N_v), their maximal length (L_{max}) and the total number of branching (N_b) have been measured. To achieve this goal, the number of intersections (N_i) of microvessels with a grid defined as the successive boundaries of the aortic ring dilated n= 1,2,3. times was considered (Figure 2a). This construction allowed taking into account the particular geometry of each set of aortic ring. The total number of intersections of microvessels (N_i) in function to the distance to the aortic ring gives the microvessel distribution. The N_i value at the first step of the grid (fixed arbitrarily at 0.01 mm to the expiant) gives N_v. The grid step at which the last $N_i \neq 0$ is measured gives L_{max}. The sum of additional intersections detected at each step of the grid gives N_b. Finally, the number of fibro-blast-like cells placed into the successive enlargement of the aortic ring limits gives N_f distribution (Figure 2b). (b) Induced-angiogenesis: each microvessel displayed a great number of branching and elongated in all directions. Consequently, in some cases the microvascular network formed a complex interconnected structure, in which the measurement of N_v, N_b and L_{max} were meaningless. Consequently, microvessel distribution has been determined.

Published in: Angiogenesis (2001), vol. 4, iss. 2, pp. 133-142
Status: Postprint (Author's version)

Figure 2. *Angiogenesis quantification in the rat aortic model by computer-based image analysis.* Panel a: determination of the microvascular outgrowth according to the vascular network complexity. The total number of intersections of microvessels (N_i) with a grid reporting to the aortic ring shape gives the microvessel distribution. The N_i value at the first step of the grid gives the number of microvessels (N_v). The grid step at which the last $N_i \neq 0$ is measured gives maximal microvessel length (L_{max}). The sum of additional intersections detected at each step of the grid gives the total number of branching (N_b). Panel b: determination of the total number of fibroblast-like cells (N_f) placed into the successive enlargement of the aortic ring limits, and their distribution.

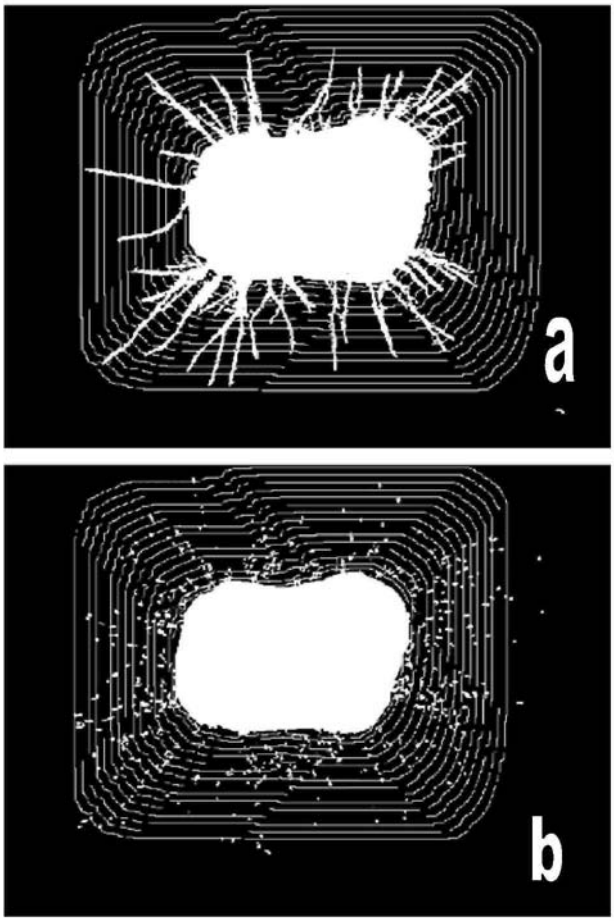

Quantification of angiogenic parameters in vascular networks of various states of complexity

Angiogenic parameters were automatically evaluated on rat aortic rings in the following situations: (a) a spontaneous angiogenic response after 5 and 10 days of culture; (b) an inhibition of neovascular outgrowth in presence of the hydroxamate-based synthetic inhibitor Batimastat; (c) a VEGF-induced angiogenesis.

From Table 1, it must be noticed that the area *A* and the factor shape *F* had almost the same value for each set of experiment. This allows asserting that results did not depend on the particular size or geometry of the aortic rings.

After 5 days of culture, aortic expiants embedded in collagen gels gave rise to capillary-like structures with isolated fibroblast-like cells, primarily confined in periaortic location (Figures 3a-c). In this case, all the parameters linked to endothelial sprouting (N_V, N_b, L_{max}), and fibroblast-like cells (N_f) can be clearly determined (Table 1). The endothelial nature of the microvessels was demonstrated by staining the aortic rings with Dil-Ac-LDL selectively taken up by endothelial cells. According to their endothelial origin, the tubular outgrowths were fluorescent whereas the individual cells were unstained (data not shown).

The complexity of the vascular network and fibroblast migration (N_i; and N_f) was more precisely studied by statistical analysis (see Material and methods section). N_i distribution had a peak ($k \cong 0$) nearby the aortic ring (d = 0.047 mm) and then decreased abruptly (sk = 0.705) (Figure 3d). This indicates that the structure was quite ordered, i.e., microvessels were short, had few branching and sprouted perpendicularly from the aortic ring. Compared to the N_i distribution, the N_f one was shifted, and had a rather flat peak ($k < 0$) centred at d = 0.125

mm and then decreased less steeply than N_i distribution (sk = 0.485). N_f reached its smallest values at distances corresponding approximately to L_{max} (Figure 3e and Table 1).

At day 10 (Figures 4a-c), the number of microvessels and their mean length reached a maximum in the aortic cultures (Table 1). N_i and N_f distributions followed almost the same trends as at day 5 (Figures 4d, e). However, at early step of the outgrowth, short and few microvessels were surrounded by a great number of fibroblast-like cells located nearby the aortic ring (Table 1). Later, microvessels increased in number (N_v = 16 ± 4 at day 5 vs. 52 ± 3 at day 10), elongated (Lmax = 0.50 ± 0.03 mm at day 5 vs. 1.20 ± 0.01 mm at day 10) and branched (N_b = 6 ± 2 at day 5 vs. 22 ± 4 at day 10). In the mean time, a dramatically decrease of $N\{$ was observed (N_f = 638 ± 185 at day 5 vs. 354 ± 38 at day 10), N_f distribution is flatter (k = -0.400 at day 5 vs. k = -1.1143 at day 10) and decreases less steeply at long distances (sk = 0.485 at day 5 vs. sk = 0.157 at day 10) (Figures 3d and 4d). However, the other statistical parameters increased between day 5 and 10, indicating that during vessel outgrowth, fibroblasts migrated at a higher distance. As observed at day 5, N_f reached its smallest values at distances corresponding approximately to L_{max} (Figure 4e and Table 1). These observations suggest that fibroblast-like cell migration delimit microvascular network.

In order to apply our quantification method to inhibitor screening, the synthetic MMP inhibitor Batimastat [15-17] was used. Quantitative analysis demonstrated a 32%, 84% and 96% range of inhibition of microvessel outgrowth in presence of 10^{-9}, 10^{-7} or 10^{-6} M (Table 1) Batimastat, respectively. Although few microvessels were observed in two out of three aortic expiants treated with 1 μM Batimastat, they were shorter (L_{max} = 0.74 ± 0.20 mm in control cultures vs. 0.19 ± 0.20 mm in Batimastat-treated cultures) and less branched (N_b = 23 ± 5 in control cultures vs. 0.5 ± 0.7 in Batimastat-treated ones) (Table 1). Thus, Batimastat affected the number, the length and the branching of vessels. However, some fibroblast-like cells retained the ability to infiltrate the surrounding matrix in the presence of the inhibitor (N_f = 397 ± 20 in control cultures vs. 189 ± 15 in the Batimastat-treated ones) (Figures 5a, b). After Batimastat treatment, N_f distribution displayed a sharp peak closer to the aortic ring (significant decrease of mean $\overline{D}$ and mode d, increase of skewness sk and kurtosis k) as compared to the control cultures (Figure 5e).

Table 1. *Computer-assisted quantification of angiogenesis in the rat aortic assay.*

Days of culture	Culture conditions	A (mm^2)	F	N_v	N_b	N_f	L_{Max} (mm)
5	Control	3.3 ± 0.2	1.25 ± 0.04	16 ± 4	6 ± 2	638 ± 185	0.50 ± 0.03
10	Control	3.6 ± 0.4	1.50 ± 0.40	52 ± 3	22 ± 4	354 ± 38	1.20 ± 0.10
8	Control	2.64 ± 0.2	1.49 ± 0.20	38 ± 3	23 ± 5	397 ± 20	0.74 ± 0.20
8	Batimastat (10^{-9} M)	3.21 ± 0.1	1.56 ± 0.20	26 ± 2	10 ± 2	405 ± 32	1.05 ± 0.20
8	Batimastat (10^{-7} M)	2.82 ± 0.1	1.55 ± 0.20	6 ± 2	0	167 ± 17	0.33 ± 0.02
8	Batimastat (10^{-6} M)	2.66 ± 0.1	1.50 ± 0.20	1.5 ± 2	0.5 ± 0.7	189 ± 15	0.19 ± 0.02
8	VEGF (5 ng/ml)	2.59 ± 0.22	1.59 ± 0.40	56 ± 3	74 ± 12	ND	1.20 ± 0.20
8	VEGF (10 ng/ml)	2.74 ± 0.38	1.95 ± 0.15	57 ± 6	81 ± 11	ND	1.25 ± 0.20
8	VEGF (20 ng/ml)	2.65 ± 0.1	1.71 ± 0.30	ND	ND	ND	ND

A - area of the projection of the aortic ring into the image; F - factor shape; N_v - number of microvessels; N_b - total number of branching; N_f -number of fibroblast-like cells; $Z_{,max}$ - maximal microvessel length; ND - not determinable. Results represent the mean value ± SD of three different sets of experiments performed in triplicate.

In order to stimulate angiogenesis exogenously and to validate the sensitivity of the proposed technique, rat aortic rings were cultured in the presence of increasing concentrations of VEGF164, a key regulator of angiogenesis [18]. From Table 1, it appears that the addition of VEGF at concentration of 5 and 10 ng/ml induced a dramatic increase of N_v, N_b, and L_{max} compared to the control. Furthermore, the interconnected network prevents N_f determination. At the highest concentration of VEGF tested (20 ng/ml), a notably increase of network complexity was observed. In this particular case, the interconnected microvessels prevented to determine accurately N_v, N_b, and L_{max}· Nevertheless, a value of L_{max}= 1.3 mm corresponding to the distance at which the last intersection was observed, has been measured. It corresponds to merely the inferior limit of the real length of the largest microvessel. In all VEGF-stimulated samples the N_i; histograms showed that the distribution broad towards the long distances and were more peaked (increase values of $\overline{D}$, sk, k, and d), compared to the control cultures. This behaviour is particularly striking for the largest VEGF concentration (Figure 5c) in which N_i increased at short distances from the aortic ring (in the range 0-0.258 mm), reached a maximum (d = 0.258 mm)

Published in: Angiogenesis (2001), vol. 4, iss. 2, pp. 133-142
Status: Postprint (Author's version)

and then decreased slowly at longer distances (in the range 0.498-1.4 mm). This kind of distribution is the signature of an interconnected network. Consequently, higher the broadness of the maximum, higher the network complexity is.

***Figure 3**. Microvascular outgrowth of rat aortic expiants after 5 days of culture.* Panels a-c: phase contrast microscopy shows that capillary-like structures and fibroblast-like cells can be clearly identified as tubular structures and isolated cells respectively (original magnification, 20x). Each photomicrograph (a-c) is representative of one of the triplicate culture performed in three different set of experiments. Panel d: determination of the number of microvessel intersections (N_i), in function of the distance to the aortic ring. Histogram has been constructed from data grouped in 15 classes. Panel e: distribution of fibroblast-like cells (N_f) around the aortic ring. Histogram has been constructed from data grouped in 20 classes. Statistical parameters are indicated for each histogram. $\overline{D}$: distance from the expiant at which N_i or N_f reach its mean value; d: distance from the expiant at which most cells migrated; sk > 0 indicates that most cells migrate at distances lower than $\overline{D}$; k: sharpness of the cell distribution around d.

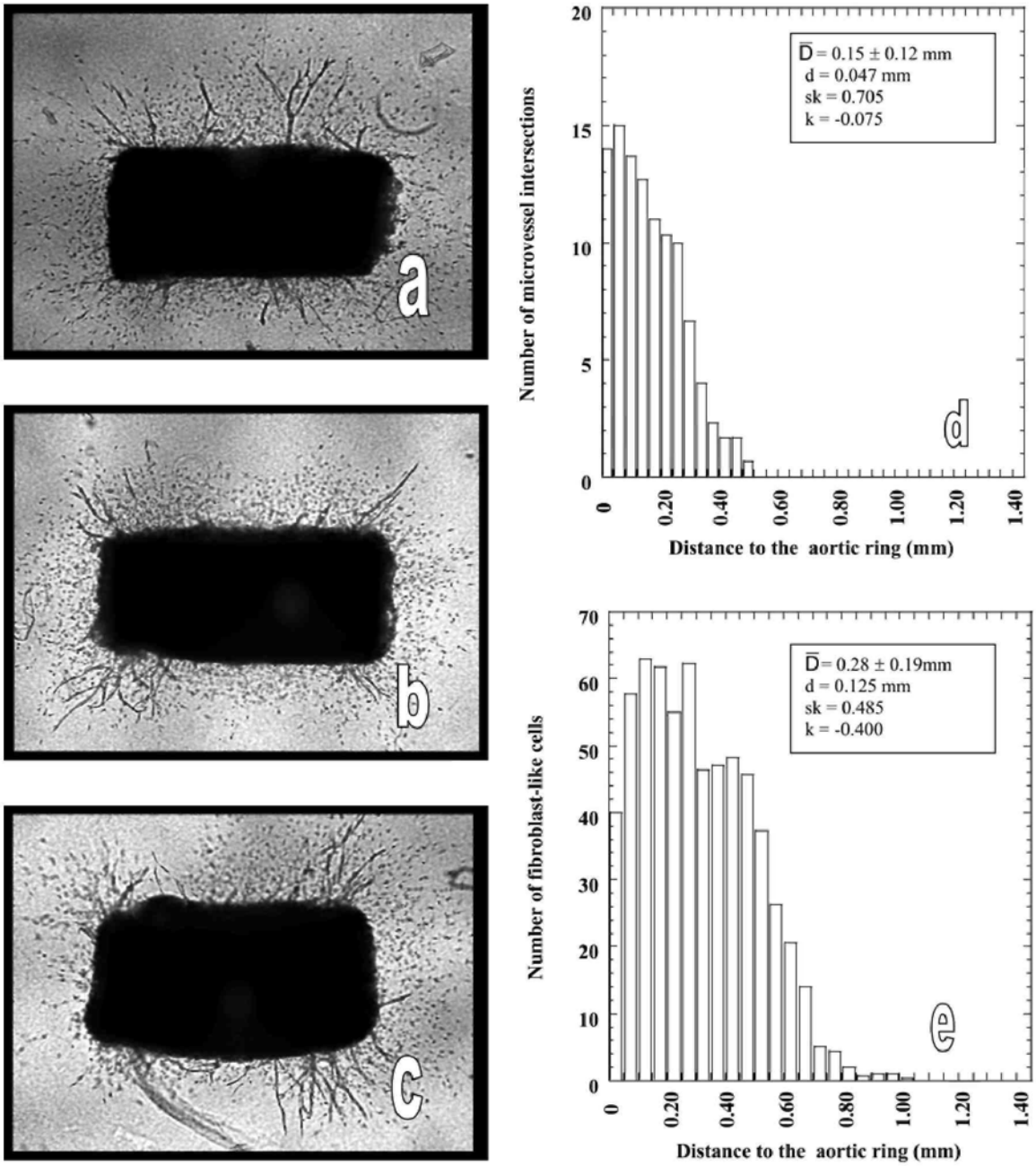

Published in: Angiogenesis (2001), vol. 4, iss. 2, pp. 133-142
Status: Postprint (Author's version)

***Figure 4**. Microvascular outgrowth of rat aortic expiants after 10 days of culture.* Panels a-c: phase contrast microscopy of three different aortic rings (original magnification, x10). Each photograph (a-c) is representative of one of the triplicate culture performed in three different sets of experiments. Panel d: determination of the number of microvessel intersections (N_i), in function of the distance to the aortic ring. Histogram has been constructed from data grouped in 15 classes. Panel e: determination of the fibroblast-like cell distribution. Histogram has been constructed from data grouped in 20 classes. Statistical parameters are indicated for each histogram. $\overline{D}$: distance from the expiant at which N_i or N_f reach its mean value; d: distance from the expiant at which most cells migrated; sk > 0 indicates that most cells migrate at distances lower than $\overline{D}$; k: sharpness of the cell distribution around d.

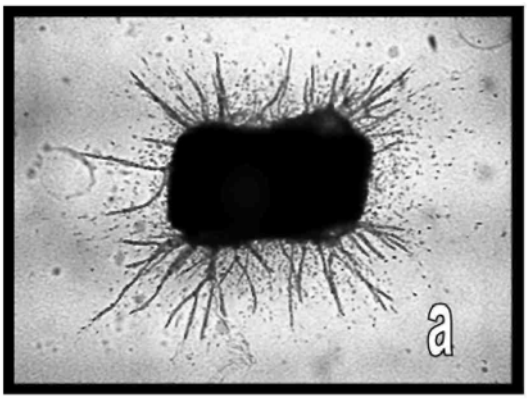

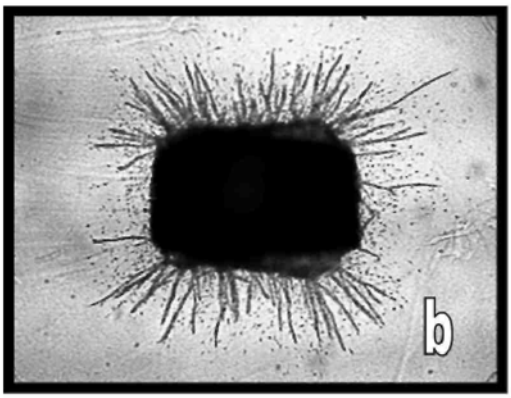

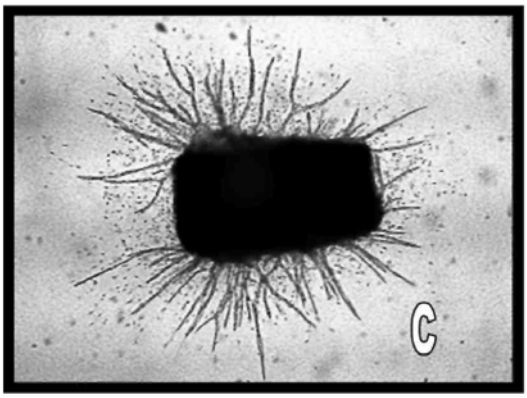

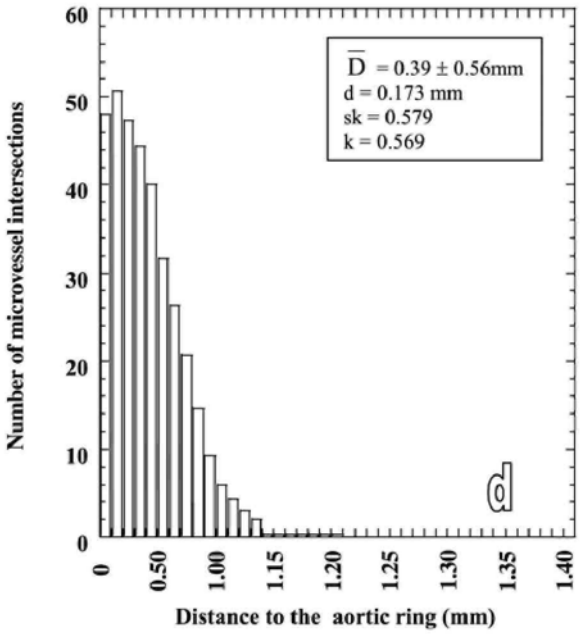

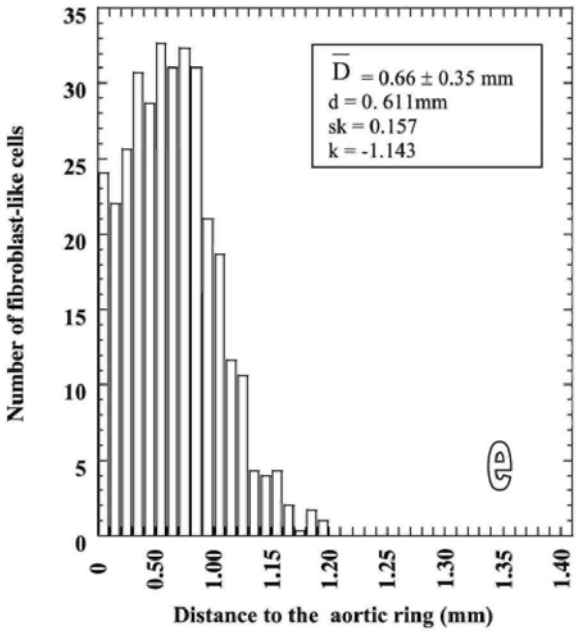

Published in: Angiogenesis (2001), vol. 4, iss. 2, pp. 133-142
Status: Postprint (Author's version)

***Figure 5**. Modulation of the microvascular network with pro- or anti-angiogenic agents.* Panels a-c: phase contrast microscopy of control (a), Batimastat (1 μM) and VEGF-treated (20 ng/ml) (c) cultures after 8 days of incubation (original magnification, xl5). Panel d: distribution of N_i in the control cultures. Histogram has been constructed from data grouped in 15 classes. Panel e: distribution of N_f in the control and the Batimastat-treated cultures. Histogram has been constructed from data grouped in 20 classes. Panel f: distribution of N_i in the VEGF-treated cultures. Histogram has been constructed from data grouped in 30 classes. Statistical parameters are indicated for each histogram. $\overline{D}$: distance from the expiant at which N_i reach its mean value; d: distance from the expiant at which most cells migrated; sk > 0 indicates that most cells migrate at distances lower than $\overline{D}$; k: sharpness of the cell distribution around d.

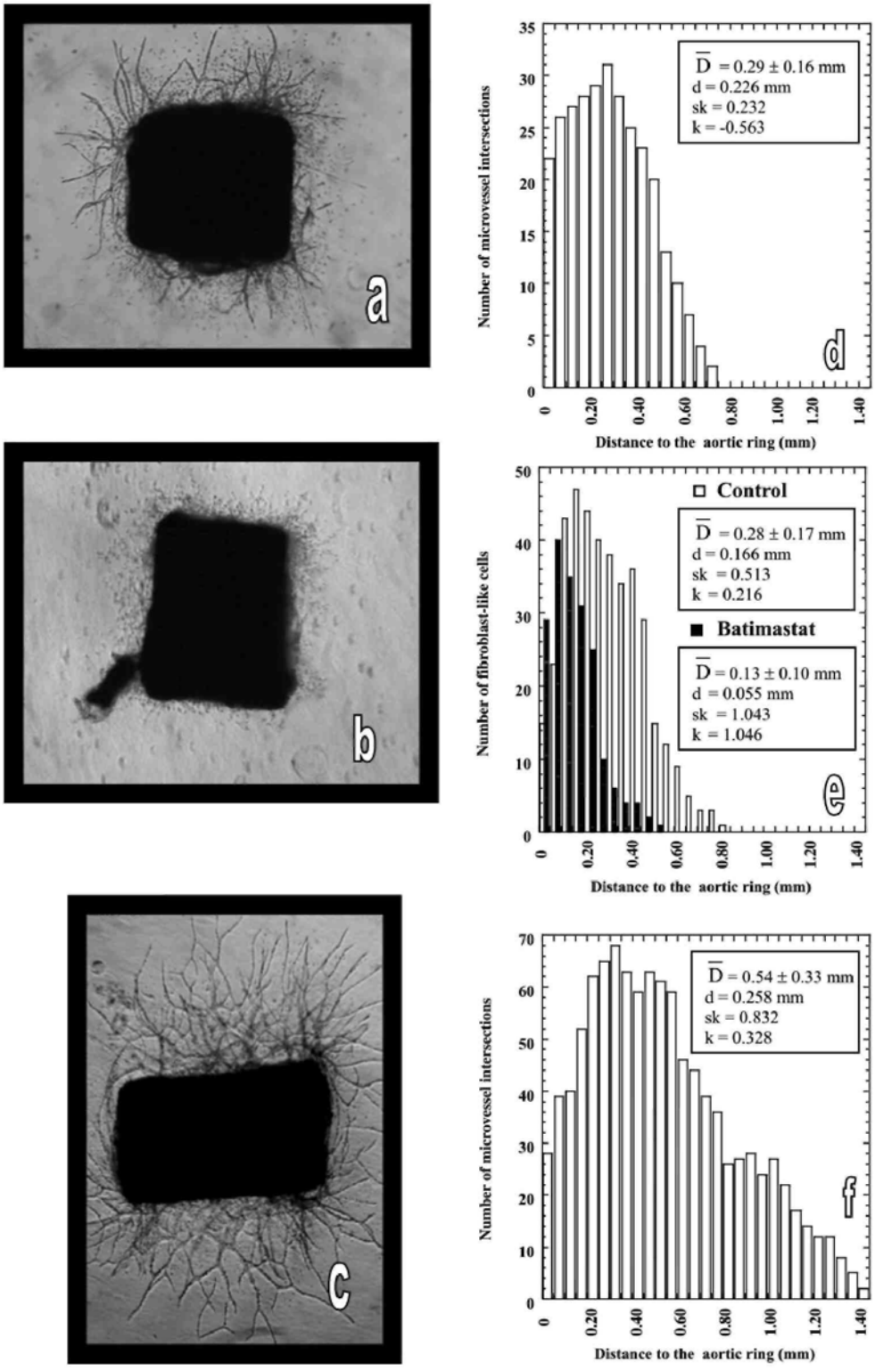

Published in: Angiogenesis (2001), vol. 4, iss. 2, pp. 133-142
Status: Postprint (Author's version)

Discussion

Since tumour growth is angiogenesis dependent [1] strategies aiming at disrupting this mechanism are heavily investigated. Several *in vitro* and *in vivo* assays [19-22] are used to directly compare the efficiency of anti-angiogenic compounds. To characterise the potential effect of these molecules, which may yield new therapeutic approaches to treat angiogenic diseases, and solid tumours, the aortic ring assay seems to be a very convenient model. Moreover, this model allows studying the spontaneous angiogenic response and the maintenance of the angiogenic process. In addition, we recently successfully adapted the aortic ring assay from rat to mice allowing the study of angiogenesis in transgenic/knock-out mice [23] (Devy et al., submitted for publication). However, quantitative methods are required to objectively quantify angiogenesis in these different models. Here, we have developed an objective automatic and reproducible method of quantification adapted to different degrees of microvascular network complexity. In this work, we show that computer-assisted image analysis is a powerful tool that allows quantifying the number, the branching, and the length of microvessels and their distributions. Moreover, the evolution of N_i with the distance to the expiant appears as an indicator of the degree of complexity of the vascular network. When microvessels grow radially, as in the spontaneous angiogenic response, N_i displays a peak closed to the aortic ring and decreases monotonically. On the contrary, when a branched structure is observed, as after VEGF-stimulation of angiogenesis, a peak of N_i appears at longer distance from the expiant. In this situation, maximal N_i value corresponds to maximal network density. Consequently, more the peak is broad, more a complex structure of intertwined branching should be expected. The present work demonstrates that the particularities of each N_i distribution can be described by statistical parameters that allow comparing various experimental situations, and characterise the network complexity.

This technique has also the advantage to allow the quantification and positioning of fibroblast-like cells. Indeed, during the kinetics of spontaneous angiogenesis a dramatic decrease in the number of fibroblast-like cells is observed. This result could be simply attributed to the limitation of the two-dimensional image capture, i.e., fibroblast-like cells are hidden by microvessel outgrowth. Alternatively, the reduced number of fibroblast-like cells as a function of the time of culture could be related to the association of these cells with new-formed vessels. Indeed, Nicosia and Villaschi [24] demonstrated that the rat aorta contains a sub-population of intimal/subintimal smooth muscle cells that differentiate into pericytes during angiogenesis *in vitro*. Interestingly, these cells have an endothelial tropism and respond to endothelial signals by contributing to the differentiation and maturation of microvessels. In the present work, quantification of microvessels development and fibroblast-like cell dispersion is in favour of this hypothesis. Our results show that during spontaneous angiogenesis, fibroblast-like cells number decrease synchronously with microvessels development, i.e., the number, the length and the branching of vessels. Moreover, the analysis of N_f distribution suggests that fibroblast-like cell migration delimits microvascular outgrowth. Altogether, these observations suggest that fibroblast-like cells do not migrate randomly, but in clear association with microvessel sprouting.

The availability of our method of quantification was assessed in cultures treated with increasing concentrations of an inhibitor of matrix metalloprotease (Batimastat) or an angiogenic agent (VEGF). The proposed technique proved to be very sensitive to morphological changes induced by both inhibition, and stimulation. Moreover, it allowed quantifying dose-dependent biological effects. Indeed, we interestingly observed a dose-dependent inhibitory effect of Batimastat on microvessel outgrowth, without completely blocking fibroblast-like cell migration. This data suggest that this inhibitor plays a specific role on endothelial cell migration and tubular morphogenesis and that fibroblast-like cell migration is likely to be limited by the inhibition of microvessel formation. We provide also evidence for a dose-dependent effect of VEGF on microvascular network complexity characterised by increased number of branchings. In this particular case, evaluation of N_i distribution appears more appropriate to quantify angiogenesis. In conclusion, our automatic image analysis coupled to the determination of different statistical parameters provides an objective method for the studies of the angiogenic process. It is well adapted to analyse vascular network complexity and allows an objective and automatic evaluation of pro- or anti-angiogenic agents. Furthermore, this new method is suitable to study endothelial and fibroblast-like cell interactions and to better understand their respective role during this complex process.

Acknowledgements

The authors also wish to thank Fabrice Olivier for its technical assistance. This work was supported by grants from the Communauté Française de Belgique (Actions de Recherches Concertées), the Commission of European Communities, the Fonds de la Recherche Scientifique Médicale, the Fonds National de la Recherche Scientifique (FNRS, Belgium), the Fédération Belge Contre le Cancer, the Fonds spéciaux de la Recherche (University of

Liège), the Centre Anticancéreux près l'Université de Liège, the FB Assurances, the Fondation Léon Frédéricq (University of Liège), the DGTRE from the 'Région Wallonne', the Fonds d'Investissements de la Recherche Scientifique (CHU, Liège, Belgium), General RE-Luxembourg, Rhône-Poulenc Rorer Pharmaceuticals (Collegeville, USA), and Roche Diagnostics GmbH (Penzberg, Germany). L.D. is a recipient of a grant from FNRS Télévie. A.N. is a Senior Research Associate from the FNRS.

References

1. Folkman J, Brem H. Angiogenesis and inflammation. In Gallin JI, Goldstein IM, Snyderman RS (eds): Inflammation: Basic Principles and Clinical Correlates. New York: Raven Press 1996; 809-39.

2. Folkman J. Angiogenesis in cancer, vascular, rheumatoid and other disease. Nature Med 1995; 1: 27-31.

3. Folkman J, Klagsbrun M. Angiogenic factors. Science 1987; 235: 442-7.

4. Auerbach R, Auerbach W, Polakowski I. Assays of angiogenesis: A review. Pharmacol Ther 1991; 51: 1-11.

5. Nicosia RF, Ottinetti A. Growth of microvessels in serum-free matrix culture of rat aorta: A quantitative assay of angiogenesis *in vitro.* Lab Invest 1990; 63: 115-22.

6. Kobayashi S, Fukuta M, Kontani H et al. A quantitative assay for angiogenesis of cultured choroidal tissues in streptozotocin-dia-betic wistar and spontaneously diabetic GK rats. Jpn J Pharmacol 1998; 78: 471-8.

7. Brown KJ, Maynes SF, Bezos A et al. A novel *in vitro* assay for human angiogenesis. Lab Invest 1996; 75: 539-55.

8. Bocci G, Danesi R, Benelli U et al. Inhibitory effect of suramin in rat models of angiogenesis *in vitro* and *in vivo.* Cancer Chemother Pharmacol 1999; 43: 205-12.

9. Kruger EA, Duray PH, Tkosos MG et al. Endostatic inhibits microvessel formation in the *ex vivo* rat aortic ring angiogenesis assay. Biochem Biophys Res Commun 2000; 268: 183-91.

10. Nissanov J, Tuman RW, Gruver LM, Fortunato JM. Automatic vessel segmentation and quantification of the rat aortic ring assay of angiogenesis. Lab Invest 1995; 73: 734-9.

11. Montesano R, Orci L, Vassali P. *In vitro* rapid organisation of endothelial cells into capillary-like networks is promoted by collagen matrices. J Cell Biol 1983; 97: 1648-52.

12. Serra J. Image Analysis and Mathematical Morphology, Vol 1. New York: Academic Press 1982.

13. Voyta JC, Via DP, Butterfield CE, Zetter BR. Identification and isolation of endothelial cells based on their increased uptake of acetylated-low density lipoprotein. J Cell Biol 1984; 99: 2034-40.

14. Himmelblau DM. Process Analysis by Statistical Methods. New York: Wiley 1970.

15. Belotti D, Paganoni P, Giavazzi R. MMP inhibitors: Experimental and clinical studies. Int J Biol Markers 1999; 14: 232-8.

16. Moses MA. The regulation of neovascularization by matrix metalloproteinases and their inhibitors. Stem Cells 1997; 15: 180-9.

17. Botos I, Scappozza L, Zhang D. Batimastat, a potent matrix metalloproteinase inhibitor, exhibits an unexpected mode of binding. Proc Natl Acad Sci USA 1996; 39: 2749-54.

18. Carmeliet P, Collen D. Role of vascular endothelial growth factor and vascular endothelial growth factor receptors in vascular development. Curr Top Microbiol Immunol 1999; 237: 133-58.

19. Benelli R, Albini A. *In vitro* models of angiogenesis: The use of Matrigel. Int J Biol Markers 1999; 14: 243-6.

20. Ribatti D, Vacca A, Wild R et al. Models for studying angiogenesis *in vivo.* Int J Biol Markers 1999; 14: 207-13.

21. Chambers AF, MacDonald IC, Schmidt EE et al. Clinical targets for anti-metastasis therapy. Adv Cancer Res 2000; 79: 91-121.

22. Jain RK, Schlenger K, HÖckel M, Yuan F. Quantitative angiogenesis assays: Progress and problems. Nat Med 1997; 3: 1203-8.

23. Carmeliet P, Moons L, Luttun A et al. Synergism between VEGF and Placental Growth Factor (P1GF) contributes to angiogenesis and plasma extravasation in pathological conditions. Nat Med 2001; 5: 75-83.

24. Nicosia RF, Villaschi S. Rat aortic smooth muscle cells become pericytes during angiogenesis *in vitro.* Lab Invest 1995; 73: 658-66.